Croatian Society for Materials Protection

Metalurgija/Metallurgy

Vol. 65 No. 3 / 2026

Effect of Thermal Aging Parameters on the Microstructure and Properties of 2024 Aluminum Alloy for Skis

Bowen Ning, Ping Hu *, Guowei Zhao, Yunpeng Zhao, Zhipeng Li

https://doi.org/10.64486/m.65.3.3

[1] Harbin Sport University, No.1 Dacheng Street, Nangang District, Harbin City, Heilongjiang Province, China, 150006; ningbowen@hrbipe.edu.cn; bowen051223@gmail.com; alice143@163.com; 18845135419@163.com; tabbli@163.com

* Correspondence: bowen051223@gmail.com

Type of the Paper: Article

Received: August 31, 2025

Accepted: December 23, 2025

Abstract: The 2024 aluminum alloy is widely used in ski manufacturing due to its high strength, good processability, and fatigue performance. However, its corrosion resistance in snowy environments remains a challenge. To address this, the present work investigates how thermal aging parameters influence the alloy's microstructure, mechanical properties, and electrical conductivity, aiming to optimize its heat treatment for ski applications. The results show that the comprehensive mechanical properties of the alloy are the best when the aging temperature is 190 °C and the thermal aging time is 10 hours. The tensile strength is 451 MPa, the yield strength is 339 MPa, the hardness is 81.3 HRB, and the conductivity is increased to 35.3 % IACS (International Annealed Copper Standard). Microstructure analysis supported by quantitative measurements shows that fine S phase (0.2–0.4) μm and θ phase are uniformly precipitated in the alloy matrix, with the highest number density and the best microstructure uniformity. These findings provide experimental basis for the optimization of heat treatment process of 2024 aluminum alloy for skis, which helps to reduce the dependence on surface protection process and improve the comprehensive performance and service life of skis.

Keywords: snowboard; 2024 aluminum alloy; microstructure; mechanical properties

1. Introduction

The performance of ski materials, as core components, critically impacts skiing experience, safety, and durability. With the growing popularity of winter sports, materials must meet stringent demands for strength, lightweight design, fatigue resistance, and corrosion resistance. Material characteristics influence ski stability in diverse snow conditions and performance during high-speed maneuvers. Among available materials, aluminum alloys are predominant in ski manufacturing due to their favorable strength-to-weight ratio, good manufacturability, and cost-effectiveness.

As a typical Al-Cu-Mg heat-treatable alloy [1-3], 2024 aluminum alloy is an ideal choice for ski plates owing to its high strength, good formability, and excellent fatigue resistance [4]. It can achieve tensile strengths exceeding 480 MPa [5] and yield strengths above 340 MPa [6], maintaining structural integrity under repeated stress, which aligns with the high demands of skiing [7-9]. Its good manufacturability also facilitates the production of complex ski geometries.

A significant limitation of 2024 alloy, however, is its susceptibility to electrochemical corrosion in ski environments containing moisture and de-icing agents [10-13]. The high copper content promotes localized pitting and oxide layer spallation, compromising both aesthetics and mechanical integrity. Current industry practices rely on surface protections like anodizing or coatings [14], but their effectiveness diminishes if the coating is damaged [15], accelerating substrate corrosion and reducing ski lifespan.

Heat treatment significantly influences the microstructure and properties of 2024 alloy [16-18]. Artificial aging can optimize precipitate morphology and distribution, enhancing mechanical performance. For instance, aging at 190 °C is known to improve strength and conductivity while reducing intergranular corrosion sensitivity [19-20]. However, detailed investigations into the effect of aging time at this temperature on the comprehensive property profile, including conductivity, are limited. This study systematically examines the influence of different aging times at 190 °C on the microstructure, mechanical properties, and electrical conductivity of 2024 aluminum alloy. The goal is to elucidate the regulation mechanism of aging parameters and provide a theoretical foundation for optimizing the heat treatment process specifically for ski applications, addressing performance needs in challenging service environments.

2. The Aging Treatment Process and Experimental Plan for 2024 Aluminum Alloy

2.1. Experimental materials and sample processing

The experimental material was a commercial 2024 aluminum alloy sheet. The chemical composition (mass fraction) of the alloy is listed in Table 1. The main alloying elements of the 2024 aluminum alloy used are Al, Cu, Mg, and other trace elements.

Table 1. Chemical composition (mass fraction, %) of the 2024 aluminum alloy

Element	Cu	Mg	Mn	Fe	Si	Zn	Ti	Cr	Al
Content/%	4.10	1.4	0.59	0.21	0.07	0.03	0.02	0.02	Bal.

The aluminum alloy sample pretreatment process used in this experiment is shown in Figure 1. Firstly, the samples were ground step by step with water-resistant sandpaper of 400 mesh to 2000 mesh (400, 600, 800, 1000, 1200, 2000 mesh in turn). Subsequently, micron-sized diamond / ethanol polishing solution was used on the polishing machine for polishing until the surface reached the mirror finish. Then, the sample was washed with anhydrous ethanol, the oil was removed by acetone solution, and the degreasing treatment was carried out again with anhydrous ethanol. Finally, the sample was dried and placed in a sealed bag for later use.

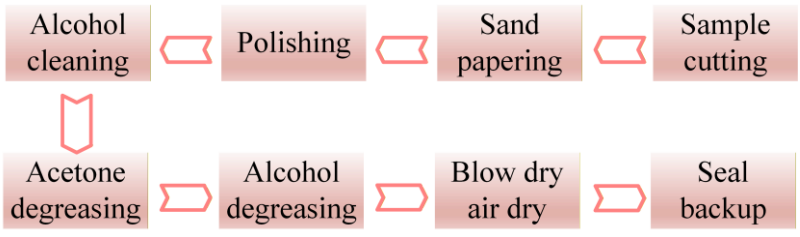

Figure 1. The sample processing flow of this experiment

2.2. Experimental materials and sample processing

Metal heat treatment can strengthen a material without changing the macroscopic size, shape and chemical composition of the material. Its essence is to improve the performance by regulating the microstructure inside the material (these structural changes usually cannot be directly observed by the naked eye). The 2024 aluminum alloy is a material that can significantly improve the mechanical properties through heat treatment. The conventional process includes natural aging or artificial aging after solution treatment. In this study, a unified

https://doi.org/10.64486/m.65.3.3

pretreatment process was adopted, that is, the samples were homogenized and annealed first, then treated at a fixed solution temperature and holding time, and finally the single-stage aging process was adopted.

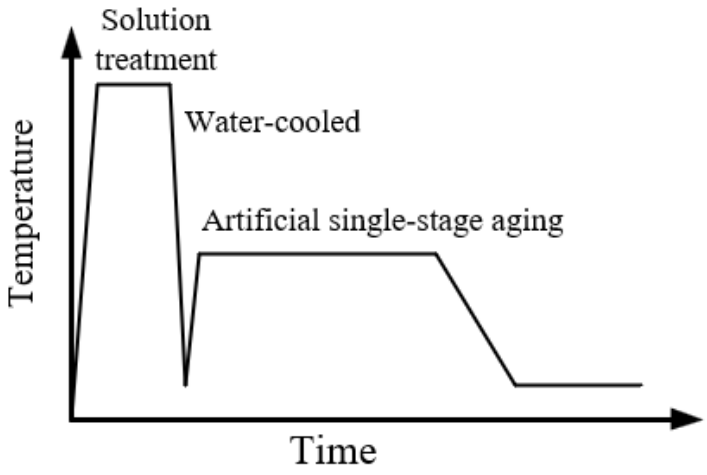

Figure 2. Heat treatment process diagram of 2024 aluminum alloy

2.2.1. Design of single-stage artificial aging experiment

The pre-treated 2024 aluminum alloy sheet was placed in a muffle furnace for solid solution treatment. The suitable solution temperature range of the alloy is 490 °C – 500 °C, and if it exceeds 505 °C, it will lead to overheating, resulting in a decrease in its mechanical properties and corrosion resistance. In this experiment, the solid solution temperature was selected as 495 °C, and the sample was placed in the furnace after the temperature was maintained for 60 minutes to ensure that the second phase was fully dissolved into the matrix.

After solution heat treatment was completed, immediate water quenching at room temperature was carried out. The quenching transfer time of the specimen transferred from the furnace to the sink is strictly controlled within 5 seconds. This is because the transfer time directly affects intergranular corrosion sensitivity, the longer the time, the higher the sensitivity.

The samples after solution treatment were initially processed and cut into plate specimens suitable for tensile test and corrosion test. After completing all heat treatment (including solution and aging), the sample is subjected to secondary finishing to reach the final size required by the national standard of tensile test. Aging treatment is carried out in an oven. According to the standard YST591-2006 ' Heat Treatment Specification for Wrought Aluminum and Aluminum Alloys ', six groups of single-stage artificial aging schemes were set up in this experiment. The temperature was 190 °C, and the holding time was from 2 hours to 24 hours (a total of six time points).

2.3. Aluminum alloy performance experiment

2.3.1. Microstructure observation

The preparation of metallographic samples strictly followed the standard metallographic experiment process. Firstly, a sample with a size of 10 mm × 10 mm × 5 mm was prepared from the center of the aluminum alloy by wire cutting. Subsequently, the grinding and polishing treatment is carried out according to the steps shown in Figure 2 until the surface reaches the mirror effect. Then, Keller 's reagent was evenly applied on the surface of the sample, and the corrosion time was controlled between 1 and 4 minutes. After the corrosion, the surface was washed with anhydrous ethanol and dried. Finally, the microstructure was observed by metallographic microscope.

2.3.2. Mechanical performance experiment

Mechanical testing and conductivity measurements were performed after aging. Tensile tests were conducted on a 5105 microcomputer-controlled electronic universal testing machine at a constant crosshead speed

https://doi.org/10.64486/m.65.3.3

corresponding to an initial strain rate of 1×10^{-3} s^{-1}. Three valid tests were performed for each aging condition. Hardness was measured on the Rockwell B scale (HRB); five indentations were taken per sample, and the average was reported. Electrical conductivity was measured using an eddy-current conductivity meter and reported in %IACS. Tensile specimens were machined via wire-electrical discharge machining according to GB/T 16865-2013 [20], with the gauge dimensions shown in Figure 3. The initial mass of each machined tensile specimen was approximately 25 g.

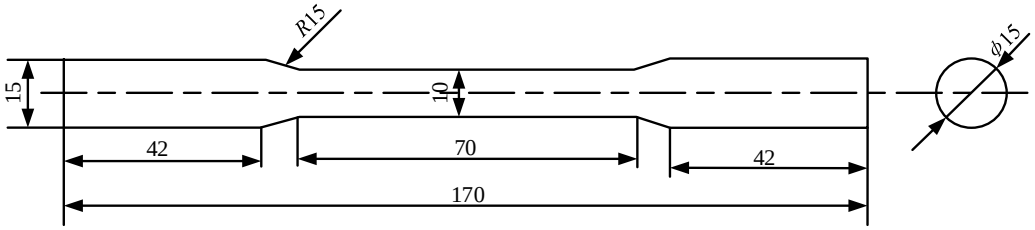

Figure 3. Processing size of tensile specimen

3. Effect of thermal aging on microstructure of 2024 aluminum alloy

Figure 4 presents separate micrographs illustrating the microstructure of 2024 aluminum alloy under different aging conditions: (a) natural aging, (b) peak aging (190 °C / 10 h), (c) overaging (190 °C / 22 h), and (d) two-stage aging. A scale bar is included in each image. The grains exhibit an elongated morphology along the rolling direction. Quantitative analysis revealed an average grain width of (45 ± 12) μm. The number density of intragranular precipitates was highest in the peak-aged condition (b), estimated at ~2.5×10^{15} m^{-2}, with an average size of 0.3 μm. Black regions are identified as impurity phases containing Fe and Mn. SEM-EDS analysis confirmed that the fine, prevalent precipitates in the peak-aged sample were enriched in Al, Cu, and Mg, consistent with the S (Al_2CuMg) and θ' (Al_2Cu) phases. The aging temperature of 190 °C was selected to promote a fine and uniform distribution of these strengthening precipitates while avoiding excessive precipitate coarsening.

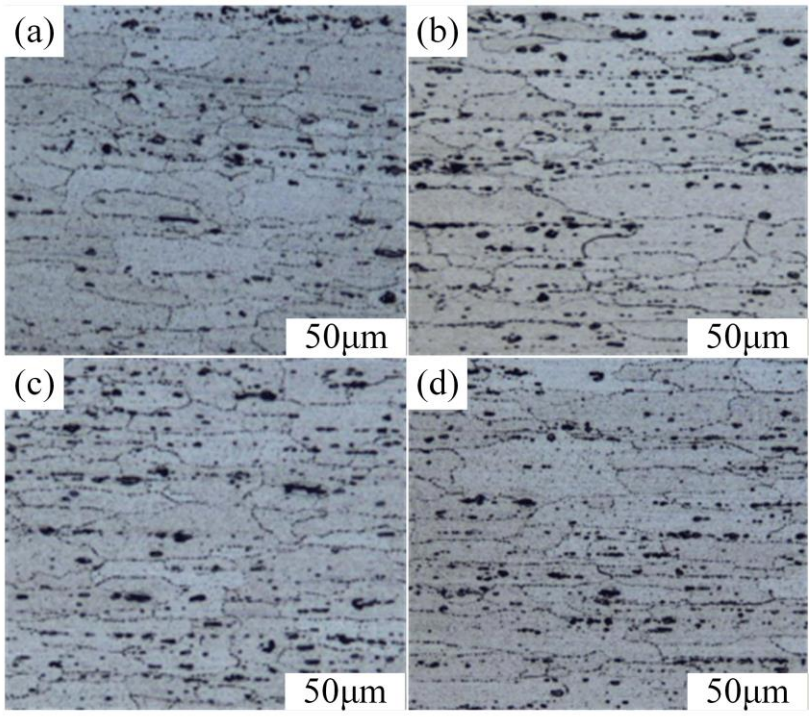

(a). natural aging, (b). peak aging, (c). over aging, (d). two-stage aging

Figure 4. Optical micrographs of 2024 aluminum alloy under different aging conditions

https://doi.org/10.64486/m.65.3.3

4. Effect of thermal aging parameters on mechanical properties of 2024 aluminum alloy

In this study, the aging temperature was set to 190 °C, and the effect of thermal aging parameters on the mechanical properties of 2024 aluminum alloy was studied. These properties include tensile strength, yield strength, elongation, electrical conductivity and hardness. The results are summarized in Table 1. For each aging condition, the measurements were repeated three times, and the results are reported as mean ± standard deviation.

Table 1. Effect of thermal aging parameters on mechanical properties of 2024 aluminum alloy (mean ± standard deviation)

No	Aging duration/h	Tensile strength/MPa	Yield strength/MPa	Elongation/%	Electric conductivity/%IACS	Hardness HRB
1	2	3	2	2	3	6
2	6	3	2	1	3	7
3	10	4	3	1	3	8
4	14	4	3	9	3	7
5	18	3	3	7	3	7
6	22	3	3	8	3	7

The hardness of the alloy was measured using the Rockwell B scale (HRB). To ensure statistical reliability, multiple indentations were made across different quadrants of each sample surface. As shown in Figure 5, the hardness of the 2024 aluminum alloy initially increases with aging time, reaches a peak at 10 hours, and subsequently decreases. This trend reflects the three characteristic stages of aging: under-aging, peak-aging, and over-aging. The observed hardness evolution is directly correlated with the precipitation behavior of strengthening phases. During the under-aging stage, the rapid increase in hardness is attributed to the formation of a high density of fine S (Al_2CuMg) and θ' (Al_2Cu) precipitates, which effectively impede dislocation motion. The peak hardness at 10 hours corresponds to the optimal microstructure, where these precipitates are uniformly distributed with the highest number density and a size of (0.2–0.4) μm. Upon further aging into the over-aging regime, the decrease in hardness results from the coarsening and reduced number density of these precipitates, which diminishes their strengthening effect.

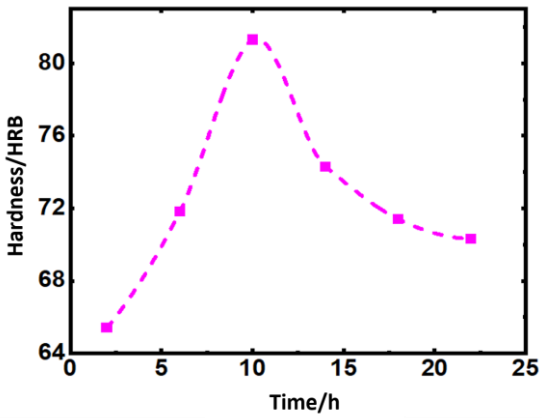

Figure 5. Effect of thermal aging parameters on the hardness of 2024 aluminum alloy

Figures 6 illustrate the variations in tensile strength and yield strength of the 2024 aluminum alloy as a function of aging time at 190 °C. Both properties exhibit trends consistent with the hardness evolution, characterized by an initial increase followed by a decrease after reaching a maximum. The optimal mechanical performance is achieved at an aging time of 10 hours, with tensile strength and yield strength peaking at 451 MPa and 339 MPa,

https://doi.org/10.64486/m.65.3.3

respectively. This strengthening behavior is closely associated with the precipitation sequence during aging. In the under-aged regime (2–10 hours), the increase in strength is attributed to the progressive formation of finely dispersed S (Al_2CuMg) and θ′ (Al_2Cu) precipitates, which act as effective barriers to dislocation glide. At the peak-aged condition (10 hours), a high density of coherent or semi-coherent precipitates with sizes around 0.2–0.4 μm provides maximal strengthening. Beyond this point, over-aging leads to coarsening and a decrease in the number density of these precipitates, reducing their ability to strengthen the matrix and consequently lowering both tensile and yield strength.

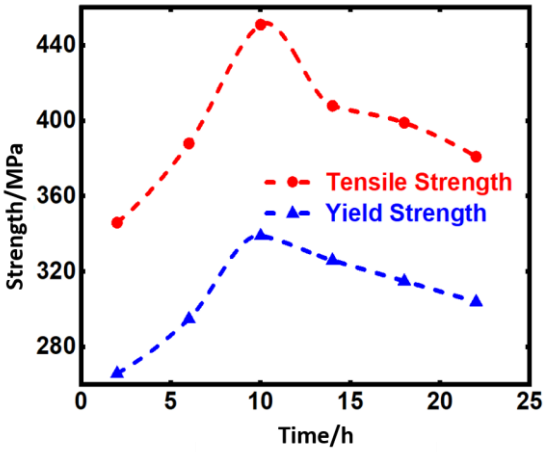

Figure 6. Effect of thermal aging parameters on tensile and yield strength of 2024 aluminum alloy

Figure 7 illustrates the variation in elongation of the 2024 aluminum alloy with aging time. As shown, the elongation after fracture decreases significantly during the initial stage of aging, followed by a more gradual decline, and exhibits a slight recovery after 18 hours.

This trend in plasticity is intrinsically linked to the microstructural evolution during aging. The rapid initial decline in elongation is attributed to the precipitation of a high density of fine S (Al_2CuMg) and θ′ (Al_2Cu) phases. These precipitates strongly impede dislocation movement, enhancing strength but concurrently reducing ductility. The slow decline around peak aging (10 hours) indicates that the precipitation process nears completion. The slight recovery in elongation observed in the over-aged regime may result from the coarsening of precipitates and an increase in inter-precipitate spacing, which facilitates easier dislocation bypass and thus a partial restoration of ductility, albeit at the expense of strength.

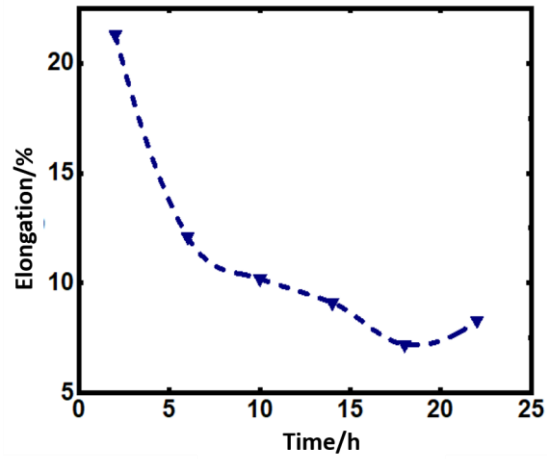

Figure 7. Effect of thermal aging parameters on the elongation of 2024 aluminum alloy

https://doi.org/10.64486/m.65.3.3

Figure 8 shows the electrical conductivity of the 2024 aluminum alloy as a function of aging time. The conductivity increases rapidly during the under-aging stage and then stabilizes after peak aging (10 hours). This trend is attributed to the depletion of solute atoms from the matrix due to precipitate formation (S and θ' phases), which reduces electron scattering.

The observed enhancement in conductivity suggests a potential improvement in stress corrosion resistance, as established in prior studies [5, 9]. Optimizing the aging process thus not only improves conductivity but may also contribute to better corrosion performance in demanding applications like skis.

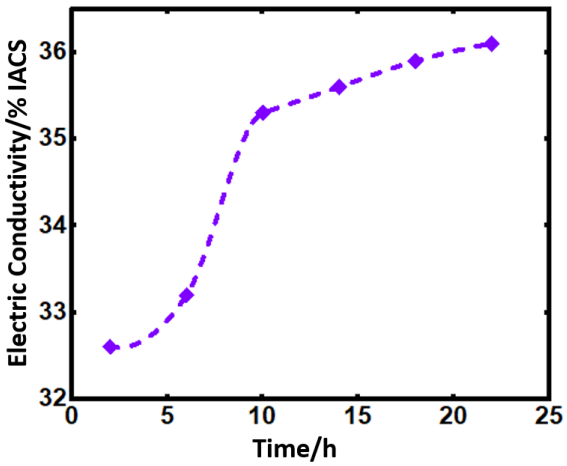

Figure 8. Effect of thermal aging parameters on electrical conductivity of 2024 aluminum alloy

5. Discussion

This study delineates the intrinsic link between aging time at 190°C, microstructural evolution, and the resulting properties of 2024 aluminum alloy. The peak performance at 10 hours represents a critical microstructural optimum.

The observed peaks in hardness, tensile, and yield strength (Figures 5 and 6) are characteristic of precipitation hardening. During under-aging (2 – 10 h), strength increases rapidly due to the formation of fine, coherent GP zones and semi-coherent S′ and θ′ precipitates [2, 6], which act as potent barriers to dislocations. This aligns with the established precipitation sequence for Al-Cu-Mg alloys [2, 7]. At peak aging (10 h), the microstructure features a uniform distribution of S and θ′ phases (~0.3 μm) with maximal number density, providing optimal strengthening via the Orowan mechanism [7]. The subsequent strength decline during over-aging (>10 h) results from precipitate coarsening (reaching 0.8 μm – 1.2 μm) and reduced number density, easing dislocation bypass, as reported in similar alloys [4, 7].

The ductility trend (Figure 6) inversely mirrors strength. The initial sharp decline is caused by strain localization around fine precipitates. The slight recovery in elongation after 18 h, concurrent with strength loss, is a known phenomenon in over-aged precipitating alloys [4] and is attributed to increased inter-precipitate spacing allowing easier dislocation glide.

The continuous rise in electrical conductivity (Figure 8) is driven by the depletion of solute atoms (Cu, Mg) from the aluminum matrix as they incorporate into S and θ′ precipitates [5, 9]. Reduced solute concentration decreases electron scattering. The stabilization post peak-aging indicates near-completion of this depletion process. The achieved conductivity of 35.3 %IACS at peak age is significant. Prior studies [5, 12] suggest a correlation between increased conductivity and improved stress corrosion resistance due to a more electrochemically homogeneous matrix with fewer solute atoms prone to selective dissolution. This implies that the optimized aging not only enhances strength but may also improve corrosion performance, a crucial factor for ski applications, though direct corrosion testing is needed for confirmation.

https://doi.org/10.64486/m.65.3.3

The optimal parameters (190 °C / 10 h) align with the T6 temper concept for 2024 alloy [2, 7], but this work precisely quantifies the property evolution with time. The findings underscore that precise aging time control is essential to tailor the microstructure for the specific high-strength and durability requirements of ski components, navigating the trade-off between strength and ductility.

5. Conclusions

Based on a systematic investigation aimed at optimizing the performance of 2024 aluminum alloy for ski core applications through thermal aging at 190 °C, the following conclusions are drawn:

(1) The optimal comprehensive mechanical properties (tensile strength: 451 MPa, yield strength: 339 MPa, hardness: 81.3 HRB) are achieved after 10 hours of aging. This is microscopically attributed to a uniform distribution of fine S and θ′ precipitates (0.2 – 0.4) μm with peak number density.

(2) Property evolution is staged: strength and hardness peak at 10 hours, while electrical conductivity increases to 35.3 %IACS, suggesting a potential enhancement in corrosion resistance due to significant solute depletion from the matrix.

(3) The recommended heat treatment process for ski applications is solid solution at 495 °C for 60 min followed by water quenching and artificial aging at 190 °C for 10 hours. This study provides a scientific basis for optimizing 2024 alloy ski components. Future work should include direct corrosion performance testing and explore the effects of minor compositional variations.

Acknowledgments: Fund: Natural Science Foundation of Heilongjiang Province, China. Fund number: JJ2023LH1583.

References

[1] X. Xiao, A. Ang, et al., "Effect of electromagnetic forming–heat treatment process on mechanical and corrosion properties of 2024 aluminum alloy," **J. Mater. Res. Technol.**, vol. 23, pp. 1027–1038, 2023. https://doi.org/10.1016/j.jmrt.2023.01.036

[2] L. Sun, L. Lu, et al., "Experimental study and optimization on solution and artificial aging of cold-rolled 2024 Al alloy sheet," *J. Mater. Eng. Perform.*, vol. 31, no. 7, pp. 5419–5431, 2022. https://doi.org/10.1007/s11665-022-06619-5

[3] Z. Wang, et al., "Nature-inspired incorporation of precipitants into high-strength bulk aluminum alloys enables lifelong extraordinary corrosion resistance in diverse aqueous environments," *Adv. Mater.*, vol. 36, no. 35, Art. no. 2406506, 2024. https://doi.org/10.1002/adma.202406506

[4] A. K. Singh, S. Ghosh, and S. Mula, "Simultaneous improvement of strength, ductility and corrosion resistance of Al2024 alloy processed by cryoforging followed by ageing," *Mater. Sci. Eng. A*, vol. 651, pp. 774–785, 2016. https://doi.org/10.1016/j.msea.2015.11.032

[5] F. E. El Garchani and M. R. Kabiri, "Intergranular corrosion and mechanical property evolution in AA2024 alloy through heat treatment," *Int. J. Adv. Manuf. Technol.*, vol. 128, no. 7, pp. 3273–3282, 2023. https://doi.org/10.1007/s00170-023-12161-y

[6] X. Xiao, et al., "Microstructure and its effect on the intergranular corrosion properties of 2024-T3 aluminum alloy," *Crystals*, vol. 12, no. 3, Art. no. 395, 2022. https://doi.org/10.3390/cryst12030395

[7] Q. Li, et al., "The effect of extrusion and heat treatment on the microstructure and tensile properties of 2024 aluminum alloy," *Materials*, vol. 15, no. 21, Art. no. 7566, 2022. https://doi.org/10.3390/ma15217566

[8] P. Campestrini, et al., "Influence of quench delay time on the corrosion behavior of aluminium alloy 2024," *Mater. Corros.*, vol. 51, no. 9, pp. 616–627, 2000. https://doi.org/10.1002/1521-4176(200009)51:9<616::aid-maco616>3.0.co;2-8

[9] H. Rivera-Cerezo, et al., "Effect of heat treatment on the electrochemical behavior of AA2055 and AA2024 alloys for aeronautical applications," *Metals*, vol. 13, no. 2, Art. no. 429, 2023. https://doi.org/10.3390/met13020429

[10] I. Guzmán-Flores, et al., "Enhancing the mechanical properties of a 6061 aluminum alloy by heat treatment from the perspective of Taguchi design of experiments," *Appl. Sci.*, vol. 14, no. 13, Art. no. 5407, 2024. https://doi.org/10.3390/app14135407

[11] D. Sarukasan and K. Thirumavalavan, "Influencing laser shock peening treatment of the mechanical, tribological, corrosion, and microstructural characteristics on AA5052 alloy," *Surf. Eng.*, vol. 40, no. 9–10, pp. 945–966, 2024. https://doi.org/10.1177/02670844241287346

[12] F. E. El Garchani, *et al*., "Effects of heat treatment on the corrosion behavior and mechanical properties of aluminum alloy 2024," *J. Mater. Res. Technol*, vol. 25, pp. 1355–1363, 2023. https://doi.org/10.1016/j.jmrt.2023.05.278

[13] H. M. Obispo, *et al*., "Copper deposition during the corrosion of aluminum alloy 2024 in sodium chloride solutions," *J. Mater. Sci*., vol. 35, no. 14, pp. 3479–3495, 2000. https://doi.org/10.1023/A:1004840908494

[14] J. Zhao, et al., "Corrosion behavior of the 2024 aluminum alloy in the atmospheric environment of the South China Sea islands," **Coatings*, vol. 14, no. 3, Art. no. 331, 2024. https://doi.org/10.3390/coatings14030331

[15] S. Sun, et al., "Long-term atmospheric corrosion behaviour of aluminium alloys 2024 and 7075 in urban, coastal and industrial environments," **Corros. Sci*.*, vol. 51, no. 4, pp. 719–727, 2009. https://doi.org/10.1016/j.corsci.2009.01.016

[16] A. A. Refeay, et al., "Effect of ageing on microstructures, electrical properties and PALS of aircraft Al alloy 2024," **Defect Diffus. Forum*, vol. 319–320, pp. 51–59, 2011. https://doi.org/10.4028/www.scientific.net/DDF.319-320.51

[17] P. Lv, et al., "Enhancement of antimicrobial properties of plasma electrolytic oxidation coatings on aluminum alloy surfaces with CuO nanoparticles," **Ceram. Int*.*, vol. 50, no. 24, pp. 55449–55460, 2024. https://doi.org/10.1016/j.ceramint.2024.10.404

[18] P. Li, et al., "Effect of post-weld heat treatment on inhomogeneity of mechanical properties and corrosion behavior of rotary friction welded 2024 aluminum alloy joint," **J. Manuf. Process*.*, vol. 75, pp. 1012–1022, 2022. https://doi.org/10.1016/j.jmapro.2022.01.059

[19] Z. Sun, et al., "Mechanical properties and corrosion resistance enhancement of 2024 aluminum alloy for drill pipe after heat treatment and Sr modification," **Mater. Today Commun*.*, vol. 36, Art. no. 106805, 2023. https://doi.org/10.1016/j.mtcomm.2023.106805

[20] L. Sun, et al., "Effects of solution and aging treatments on the microstructure and mechanical properties of cold rolled 2024 Al alloy sheet," **J. Mater. Res. Technol*.*, vol. 12, pp. 1126–1142, 2021. https://doi.org/10.1016/j.jmrt.2021.03.051